



ELSEVIER

Contents lists available at ScienceDirect

Computers in Biology and Medicine

journal homepage: www.elsevier.com/locate/cbm

Feasibility of quantitative analysis of regional left ventricular function in the post-infarct mouse by magnetic resonance imaging with retrospective gating

Matteo Franzosi^a, Uliano Guerrini^a, Laura Castiglioni^a, Luigi Sironi^{a,b}, Elena Nobili^{a,b},
Elena Tremoli^{a,b}, Enrico G. Caiani^{c,*}

^a Dipartimento di Scienze Farmacologiche, Università degli Studi di Milano, Milan, Italy

^b Centro Cardiologico Monzino—IRCCS, Milan, Italy

^c Dipartimento di Bioingegneria, Politecnico di Milano, Milan, Italy

ARTICLE INFO

Article history:

Received 5 July 2010

Accepted 30 June 2011

Keywords:

Myocardial infarction

Mice model

Left ventricle regional analysis

Magnetic resonance imaging

Retrospective gating

Regional fractional area change

ABSTRACT

We aimed testing feasibility of identification of regional left ventricular (LV) endocardial motion abnormalities in mice undergoing coronary ligation (MI), using cine magnetic resonance with retrospective gating and computation of regional fractional area change (RFAC), by comparison with histological “gold standard” evaluation. ROC analysis determined the optimal RFAC cut-off values for detecting regional ischemic injury. This approach was tested on 18 MI and 10 sham mice. Automated regional LV motion interpretation and bull’s eye display allowed non-invasive localization of the induced infarction. Possible applications to future studies assessing the effectiveness of pharmacological treatments or regenerative medicine are expected.

© 2011 Elsevier Ltd. All rights reserved.

1. Introduction

Cardiovascular disease is one of the leading causes of morbidity and mortality in industrialized countries [1]. Despite considerable advances in diagnosis and management over the last 30 years, acute myocardial infarction is the most frequent cause of death (30%) in the adult population of Western countries, where almost all infarctions are due to the acute coronary occlusion caused by atherosclerotic plaques.

Acute myocardial infarction has been mimicked in a variety of rat and mouse models. Among these, the murine model of myocardial infarction (MMMI) has been extensively studied as a means of clarifying the functional, structural and molecular changes associated with clinical ischemic heart disease, and testing the effectiveness of new pharmacological therapies [2]. In this context, the precise evaluation of the degree and extent of myocardial injury after an acute ischemic event is needed to interpret correctly the physiological results.

However, *in vivo* evaluations of the MMMI rely on imaging technologies (ultrasound, micro-X ray computed tomography, magnetic resonance imaging) that are each characterized by a number of limitations in spatial and temporal resolution, and constrained by the unique aspects of mouse physiology and size.

In particular, non-invasive imaging methods like echocardiography and magnetic resonance (MR) imaging are very valuable in longitudinal follow-up studies of cardiac function in small animals. High-frequency echocardiography (hf-echo) M-mode is easy to apply, has high temporal and spatial resolution, and good reproducibility. However, the assessment of LV volumes is performed transforming 1-D measurements by geometric formula. Self-gated MR might be advantageous in cases of abnormal LV geometry and heterogeneous regional myocardial function, as it is expected after myocardial infarction provoked by coronary ligation, as LV volume computation is based on contiguous 2D chamber area measurements [3].

MR imaging is the method of choice for the left ventricular (LV) volumetric quantification of cardiac function in mice [4–6], but its use is limited by several factors: (1) animal sedation and hyperthermia, which may interfere with cardiac function; (2) the high heart rate of about 600 bpm that precludes the use of the fast sequences used in humans; (3) the presence of rhythm disturbances and respiratory variability, which lead to gating problems and longer acquisition times: as MR image sampling is usually synchronised with the cardiac cycle (cardiac ECG triggering) and interrupted during respiratory activity (respiratory gating), acquisition time is approximately 7–10 min/slice.

In order to address some of these limitations, an imaging approach based on a gradient echo sequence and retrospective gating by a non-spatially encoded navigator for every acquired echo can be applied (Intragate, Bruker). It allows cardiac images

* Corresponding author.

E-mail address: caiani@biomed.polimi.it (E.G. Caiani).

to be obtained without ECG or respiratory gating, and its feasibility and related advantages for murine cardiac MRI have been previously described [7–9].

From cine MR images, it is possible to determine global indexes of LV function, such as end-diastolic (EDV) and end-systolic (ESV) volumes, ejection fraction (EF), stroke volume (SV) and LV mass [4–6,10,11]. However, in order to obtain information on LV regional function, that could be useful in the assessment of the effectiveness of focused pharmacological treatments or regenerative medicine in MMMI, particular acquisition procedures, like tagged cardiac MR and harmonic phase (HARP) tracking [12], displacement encoding via stimulated echoes (DENSE) [13], can be applied. MR tagging allows the measurement of the displacements of material points (i.e., nodes of a grid) overimposed to the myocardial tissue by a localized deformation of the magnetization. DENSE represents a phase contrast method that has the ability to extract myocardial motion data at high spatial density over segments of the cardiac cycle. These two modalities represent the current gold standard of 3D strain analysis, from which direct and highly sensitive measures of intra-myocardial strain throughout the heart can be computed.

However, these techniques are limited by the increase in the imaging acquisition time [14] that augments the animal stress, thus resulting in the acquisition of a reduced number of slices over the entire LV [15].

We hypothesized that temporal and spatial resolution achieved by cine MR with retrospective gating could be sufficiently high to allow the quantification of not only global indices of LV function, but also of frame-by-frame regional LV areas, from which automatically detect endocardial wall motion abnormalities.

Accordingly, the aim of this study was to test the feasibility of using cine MR images with retrospective gating to identify regional LV endocardial motion abnormalities in MMMI, using semi-automated quantification analysis tools. To do so, we proceeded as follows: (1) a “gold standard” for LV regional wall motion interpretation was obtained by analysis of histological samples from a sub-group of 7 mice after selective left anterior descending (LAD) coronary ligation; (2) in these animals, from MR images regional fractional area change (RFAC) was quantified, and receiver operating characteristic (ROC) analysis was performed referring to the histological analysis, to determine the optimal regional RFAC cut-off value for achieving the highest accuracy in automated wall motion interpretation; (3) to verify the reliability of the selected thresholds, they were applied to a control group (C) consisting of 10 sham-operated mice, to test their accuracy in interpreting true and false negative; (4) the selected thresholds were applied to additional 18 mice with selective LAD coronary ligation, in order to describe the extent of the provoked ischemia on global and regional LV function and mass.

Obtained results with the proposed methodology support the hypothesis that MR imaging with retrospective gating can be utilized for an expedited 2D analysis of regional LV wall motion abnormalities.

2. Methods

2.1. Animals and surgical procedures

Female C57BL6 mice aged 6–8 weeks and weighing 20–25 g were purchased from Charles River Laboratories (Calco, Italy). The procedures involving animals and their care respected our institutional guidelines, which comply with national and international law and policies (4D.L. N.116, G.U., supplement 40, 18-2-1992; EEC Council Directive 86/609, OJ L 358,1,12-12-1987; National Institutes of Health's Guide for the Care and Use of Laboratory

Animals and US National Research Council 1996), and every effort was made to minimize the number of animals used and their suffering.

The MMMI group consisted of 37 mice in which myocardial infarction was induced by means of the permanent ligation of the LAD coronary artery. Briefly, anesthetised mice (75 mg/kg ketamine and 0.05 mg/kg medetomidine) were intubated via the trachea with a steel tube and ventilated with positive airway pressure (a breathing volume of 140 μ l at 150 breaths/min) [16]. Left thoracotomy (with dissection at the fourth intercostal space) exposed the antero-lateral heart surface, and myocardial infarction was induced by ligating the LAD coronary artery at the level of its bifurcation using 7.0 nylon threads. During surgery, body temperature was maintained constant at 37.5 °C by means of a heating carpet. The operation took approximately 30 min, after which the thorax was closed and the animal was extubated and monitored. The medetomidine antidote atipamezolo (0.05 mg/kg) was administered to encourage animal awakening.

The C group consisted of 10 sham-operated mice.

2.2. In vivo MR imaging

Nine days after surgery, the mice were anesthetised with inhaled isoflurane (1.5–2 vol%, in a 30/70 oxygen–nitrogen saturated chamber), fixed on a holder and placed into a 3.8 cm diameter birdcage coil. Isoflurane subadministration was maintained also during image acquisition.

The images were recorded using a 4.7 T vertical-bore MR magnet (Bruker) and a gradient echo cine sequence with the following parameters: echo time 1.9 ms; repetition time 10 ms; field of view 4 × 4 cm²; acquisition matrix 128 × 128 pixels; slice thickness 1 mm. During image acquisition, the mice temperature was monitored rectally.

The MR data were acquired in multiple contiguous short-axis slices, using 12 frames for every cardiac cycle. The planes corresponding to the slices to be acquired (orthogonal to the long-axis of the heart) were selected on a T1-weighted scout image, and an additional slice was defined in order to position the free induction decay (FID) navigator.

The images were acquired based on a gradient echo sequence with a non-spatially encoded FID (Intragate, Bruker) for every acquired echo [8]. By this technique, the module and phase of the FID signal, together with their derivatives, are combined in order to obtain a time-dependent signal that provides information for the retrospective reconstruction of high quality cardiac cine images even in the presence of considerable variations in respiratory and/or cardiac rates. From this FID signal, also an estimate of the mean heart rate during image acquisition was obtained.

2.3. Histological analysis

One hour after the conclusion of the MR imaging, a sub-group of 7 mice from the MMMI group was anesthetized (75 mg/kg ketamine and 0.05 mg/kg medetomidine), the abdominal aorta was cannulated, the heart was arrested in diastole with CdCl₂ and the myocardium was perfused with PBS fixed in 4% phosphate-buffered formalin for 24 h and embedded in paraffin; then 20 μ m axial sections (from base to apex) were prepared. After deparaffination and rehydration, sections were stained with hematoxylin and eosin. For each MR slice, a corresponding section was selected and acquired with a high-resolution digital camera using 1:1 macro-lens. Digital planimetry was performed to detect scar tissue based on different colorization due to hematoxylin and eosin staining.

In order to determine the “gold standard” for wall motion interpretation, in these images the LV cavity was manually

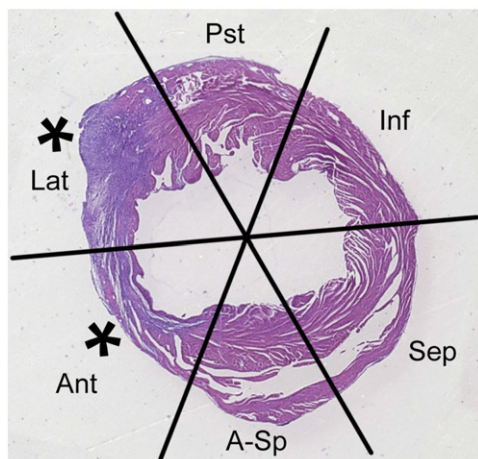


Fig. 1. Example of a histological sample at mid-apical level, obtained from an ischemic mouse after being processed for hematoxylin and eosin staining, with superimposed the 6-sectors (Sep: septal, A-Sp: antero-septal, Ant: anterior, Lat: lateral, Pst: posterior, Inf: inferior) division scheme utilized for regional evaluation. The “*” indicates segments classified as abnormal (see text for details).

divided into six 60° sectors (anterior, antero-septal, septal, lateral, posterior and inferior) based on the position of the junction between the right ventricular free wall and the interventricular septum. Each segment was classified as abnormal (ischemic) if the percentage of scar tissue contained in each sector was more than 50% of the relevant myocardium. Otherwise, it was classified as normal (Fig. 1).

2.4. MR image analysis

The MR Dicom images were analyzed using custom software implemented in the Matlab environment (The Mathworks Inc., Natick, MA), with the images being cropped by manually selecting a region of interest surrounding the LV on the end-diastolic frame.

In each slice, the endocardial border was semi-automatically detected frame-by-frame throughout the cardiac cycle using a local thresholding technique [17], in which the thresholding parameters are manually optimized for the first frame and then adjusted when necessary for the rest of the sequence. Fig. 2a schematizes the procedure, showing the end-diastolic (outer contour, in blue) and end-systolic (inner contour, in green) endocardial borders superimposed to the original image in a healthy mouse. Once the endocardial border was detected, the area of the LV cavity was computed as pixel counts and expressed in squared micrometers. In order to obtain global indices, the LV volume for each frame was computed as the sum of the LV cavity areas in each slice multiplied by the slice thickness, and the LV volume versus time curve was used to define ESV and EDV, respectively, as its minimum and maximum. SV and EF were computed, and derivation of the LV volume curve resulted into the rates of peak filling (PFR) and peak ejection (PER) as the absolute maximum and minimum, respectively.

LV mass was obtained by first manually tracing the epicardial border on the end-systolic frame of each slice (Fig. 2a, second row, outer contour – in red), and then taking the sum of the differences between the epicardial and endocardial areas, multiplied by the slice thickness and myocardial tissue density (assumed to be 1.05 g/cm^3) [18].

For the quantitative analysis of regional endocardial wall motion, similarly to the images of the histological samples, the LV cavity was divided into six 60° sectors (anterior, antero-septal, septal, lateral, posterior and inferior) using its centroid, which was automatically calculated on the end-systolic frame of each slice,

and an additional point manually placed at the junction between the right ventricular free wall and the interventricular septum. By automatically repeating these operations frame-by-frame for each sector, regional LV chamber area was computed and expressed as a % of regional end-diastolic area (rEDA). The regional fractional area change (RFAC) in the % of rEDA was then computed and used as index of regional endocardial wall motion (Fig. 2b) [17].

Moreover, regional LV thickness was obtained by tracing 18 concentric rays (one every 20°) from the cavity centroid on the end-systolic frame of every slice, and measuring the mean distance between the endocardial and epicardial borders along three consecutive rays (Fig. 2c).

To allow an easy visualization of the results of regional LV wall motion and wall thickness of the entire ventricle in a single image, the RFAC and LV thickness were displayed in a “bull’s eye” format in which the red tones represent lower and the green tones higher values. The inner circle represents the LV apex, and the outer rings consecutive slices from the apex to the base.

2.5. Statistical analysis

In order to test the reliability of MR with retrospective gating in providing information useful for automated regional wall motion interpretation, we proceeded as follows: (1) for each sector (anterior, antero-septal, septal, lateral, posterior and inferior), ROC analysis was computed by comparing the histological interpretation obtained in the sub-group of 7 mice with the RFAC results obtained from the corresponding MR images by counting the segments where concordant (true positive and negative) as well as discordant (false positive and negative) readings were made. Segment counts were used to calculate the sensitivity, specificity and overall accuracy for each RFAC abnormality threshold; (2) for each sector, the optimal RFAC cut-off value for automatically interpreting a segment as normal or abnormal (ischemic), according to the histological, was determined as the value providing the highest accuracy; (3) to further verify the reliability of the selected regional thresholds, they were applied to the C group, to test their accuracy in interpreting true and false negative.

These values were then utilized to automatically detect the abnormal segments in the remaining mice of the MMMI group, to describe the extent of the effects of the coronary ligation on regional LV function.

To allow the averaging of RFAC and LV thickness in mice with a different number of slices covering the LV, the values from different slices in each mouse were resampled using cubic spline interpolation to obtain 10 values for each of the six sectors. These values were then averaged on a point-by-point basis to obtain mean RFAC \pm SD and mean LV thickness \pm SD every 10% of LV length from the base to the apex. This process was used for all the mice of both the MMMI and C groups, and allowed testing for differences in each 10% of LV length (unpaired *t*-test, *: $p < 0.05$).

3. Results

Of the 37 mice undergoing LAD ligation, 11 died due to complications during surgery or post-surgery, and 1 died during the MR acquisition (67% survival rate). All sham mice survived the operation. The use of the Intragate sequence allowed to acquire a single slice in a timeframe of 2–3 min only, thus causing less stress to the animal. An average of 7 and 5 slices were acquired in MMMI and C, respectively.

Table 1 shows the measurements of the LV global parameters computed in the MMMI and C group: as expected, in MMMI the

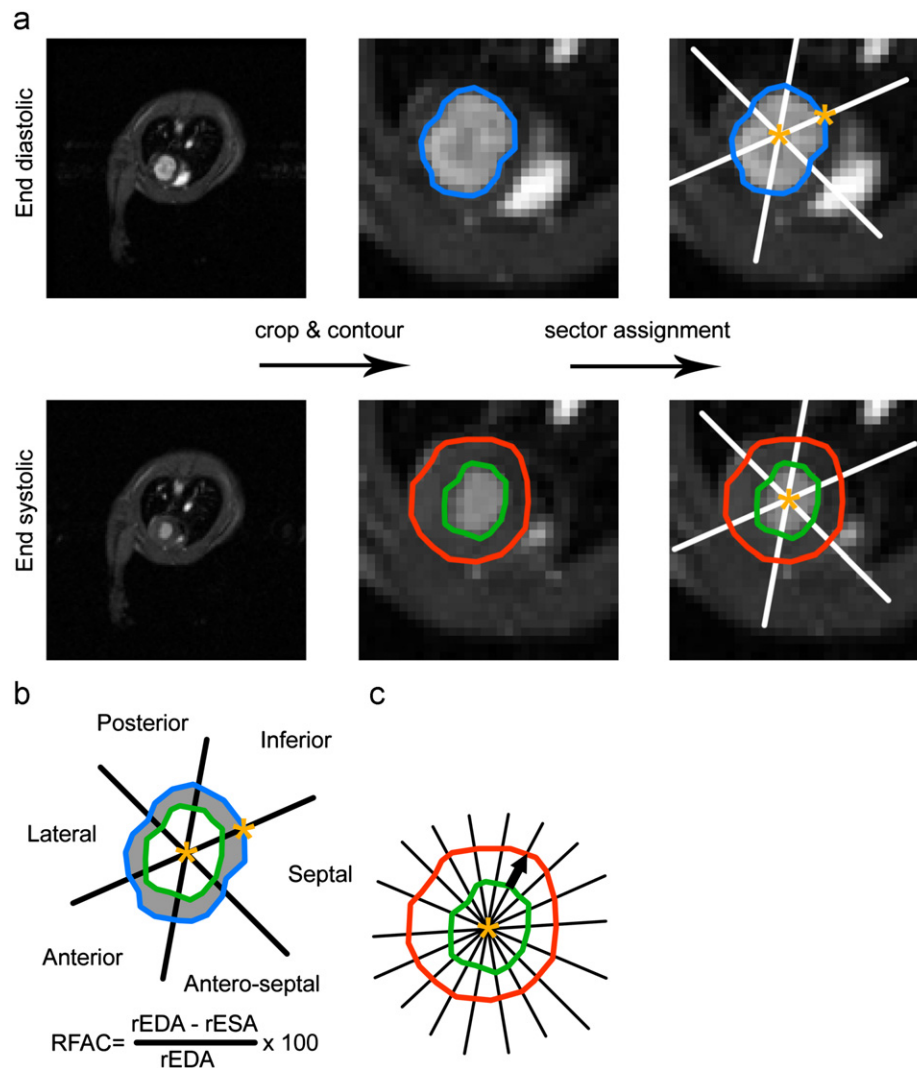


Fig. 2. (a) Example of the acquired MR images in a healthy mouse at end diastole (left-top panel) and end systole (left-bottom panel). After image cropping in order to include the LV cavity, the LV endocardial contour was detected frame-by-frame using a semi-automated software for border detection (top row – in blue, and second row, inner contour – in green). Moreover, on the end-systolic frame, the epicardial border was manually traced for LV mass and wall thickness evaluation (second row, outer contour – in red). (b) Schematic representation of the computation of regional fractional area change in a short-axis slice of the left ventricle. Following endocardial border detection, the LV cavity was divided into six 60° wedge-shaped sectors, from which regional areas were computed frame-by-frame. End-diastolic (rEDA, outer contour – in blue) and end-systolic (rESA, inner contour – in green) regional areas were used to calculate regional fractional area change (RFAC), expressed in % of rEDA. (c) Schematic representation of regional LV thickness: for every slice at the end-systolic frame 18 concentric rays (one every 20°) were traced from the cavity centroid. Regional LV thickness was measured as the mean distance between the endocardial and the epicardial border (black arrow in the bottom center panel) along three consecutive rays, using the same division scheme used for regional function. (For interpretation of the references to color in this figure legend, the reader is referred to the web version of this article.)

Table 1
Global LV parameters in controls (C) and infarcted mice (MMMI).

	C	MMMI
HR (bpm)	431 ± 72	425 ± 71
EDV (μL)	36 ± 4	92 ± 25*
ESV (μL)	10 ± 3	66 ± 27*
SV (μL)	26 ± 3	26 ± 4
EF (%)	72 ± 7	31 ± 10*
LV mass (mg)	77 ± 8	96 ± 23*
PFR (a.u.)	3.6 ± 0.4	1.9 ± 0.5*
PER (a.u.)	−3 ± 0.5	−1.8 ± 0.8*

* $p < 0.05$ (unpaired t -test); EDV: end-diastolic volume; ESV: end-systolic volume; SV: stroke volume; EF: ejection fraction; PFR: peak filling rate; PER: peak ejection rate.

LV size and mass were increased in respect to C, together with a lower EF, PFR and PER. HR was not different between the two groups.

The calculation of RFAC was fully automated and required < 1 min per mice (2 GHz Pentium-4 personal computer Dell Inc., Round Rock, TX), once the endocardial borders were detected and the anatomic landmarks required for segmentation were set, which took 30 s to 4 min per slice depending on the quality of endocardial visualization and the presence of the papillary muscles in that particular slice.

According to the histological interpretation of the 7 mice studied by histology (6 or 7 slices per animal corresponding to the acquired MR slices), 270 segments were classified: 164 (71%) as normal and 106 (39%) as ischemic (abnormal). The corresponding results of the ROC analysis are reported in Table 2. Different RFAC cut-off values were found for each of the six sectors, with higher values associated to anterior and lateral sectors. Using these threshold values, the automated interpretation based on RFAC computed from the MR images showed normal RFAC in 145/270 sectors (54%) and abnormally reduced RFAC in the remaining 125/270 sectors (46%). This interpretation disagreed

with the “gold standard” in 37/270 segments (14%), of which 17 were false positive, and 20 were false negative.

When applied to the C group, these regional thresholds resulted in 6/306 false positives (2%), thus evidencing an optimal accuracy (98%) in correctly interpreting segments with normal wall motion.

Fig. 3 shows the regional chamber area curves (expressed as a % of rEDA) obtained in the six sectors of one mid-LV slice in a C and MMMI mouse. The general shape of the curves (particularly

in the control) reflects on a regional basis the expected changes in LV area throughout the cardiac cycle, including systolic contraction and the subsequent diastolic filling phases (rapid filling, diastasis and atrial contraction). As expected, in the MMMI mouse, the peak-to-peak amplitude (i.e. RFAC) seems to be depressed in the sectors most affected by LAD ligation. The regional heterogeneity of RFAC in C group, and the total extent of the induced LV infarct in the MMMI mice, can be seen in the corresponding bull's eye representations, where segments automatically classified as abnormal are represented with bold black contours.

Figs. 4 and 5 show the mean RFAC and mean LV thickness, respectively, obtained in the 10 C mice (gray squares) and 18 MMMI mice (black dots) every 10% of LV length from the base to the apex. In Fig. 4, it is worth noting that the curves showed a trend towards an increase in RFAC from the base to the apex in the C mice, but a progressive decrease in the MMMI mice, thus leading to significantly lower values in the anterior, posterior and lateral sectors throughout the LV. In the antero-septal, septal and inferior sectors, this reduction was significant only at the mid- and apical-level. Fig. 5 shows a significant reduction in regional LV thickness from base to apex only in the anterior sector of the MMMI mice; in the other sectors, it was significant only at the mid-apical or apical level.

Table 2

Results of ROC analysis applied to each of the six regional sectors (Sep=septal, A-Sp=antero-septal, Ant=anterior, Lat=lateral, Pst=posterior, Inf=inferior) in which the left ventricle has been divided (FN=false negative, FP=false positive, TP=true positive and TN=true negative).

	RFAC % Cut-off	Accuracy	Specificity	Sensitivity	FN	FP	TP	TN
Sep	26	82	94	54	6	2	7	30
A-Sp	26	80	77	84	3	6	16	20
Ant	47	93	85	97	1	2	31	11
Lat	46	93	87	97	1	2	28	14
Pst	31	89	89	88	2	3	15	25
Inf	23	80	93	61	7	2	11	25

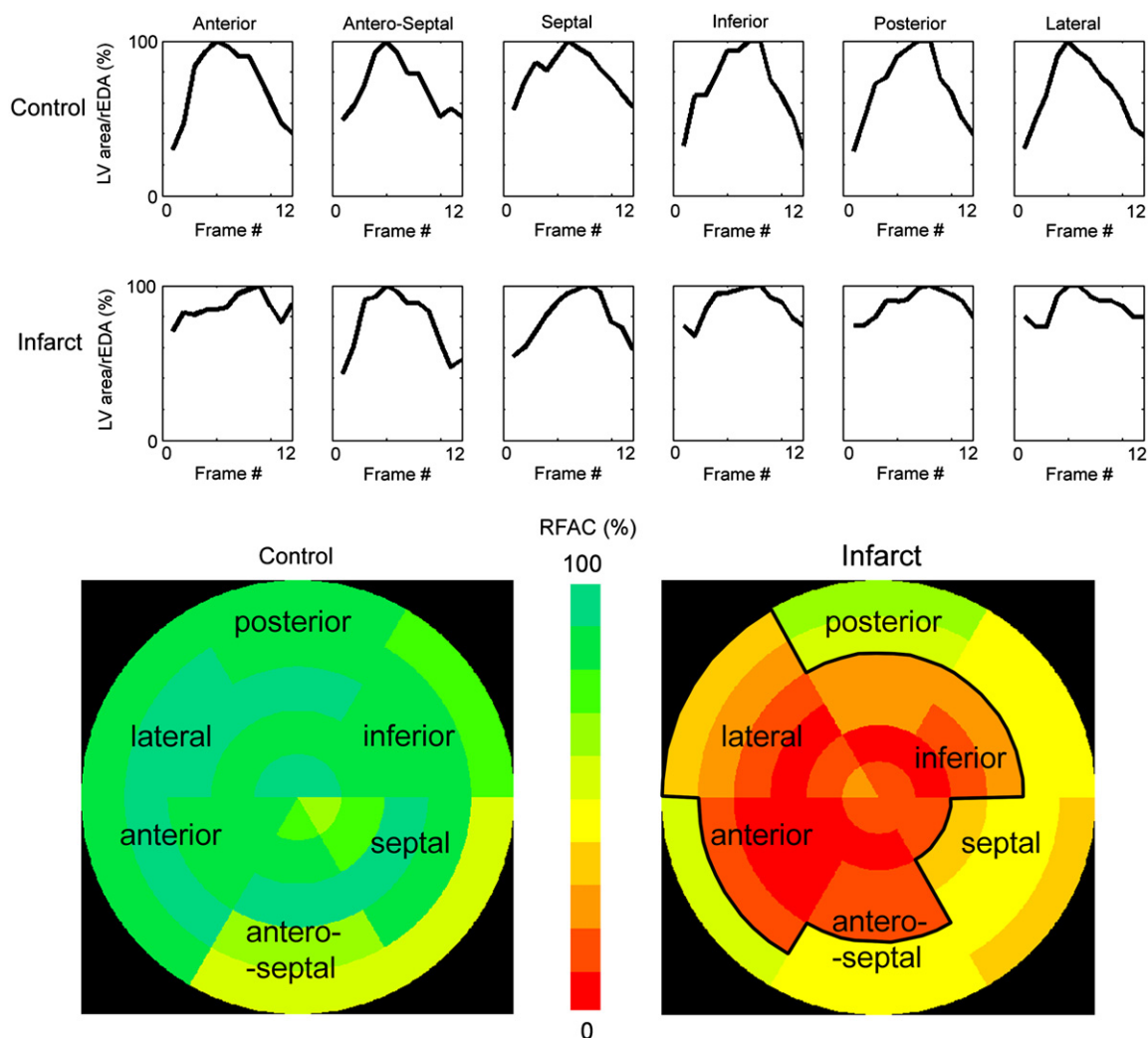


Fig. 3. Regional fractional area curves (RFAC) as % of regional end-diastolic area (rEDA) throughout the cardiac cycle, measured in a control (C, top) and in an infarcted mouse (MMMI, bottom) at mid-basal level in the six LV sectors. Also, the corresponding RFAC ‘bull’s eye’ displays are shown (C, left and MMMI, right). Bold black contour on the ‘bull’s eye’ evidences those sectors in which the RFAC values were lower than the corresponding regional cut-off thresholds.

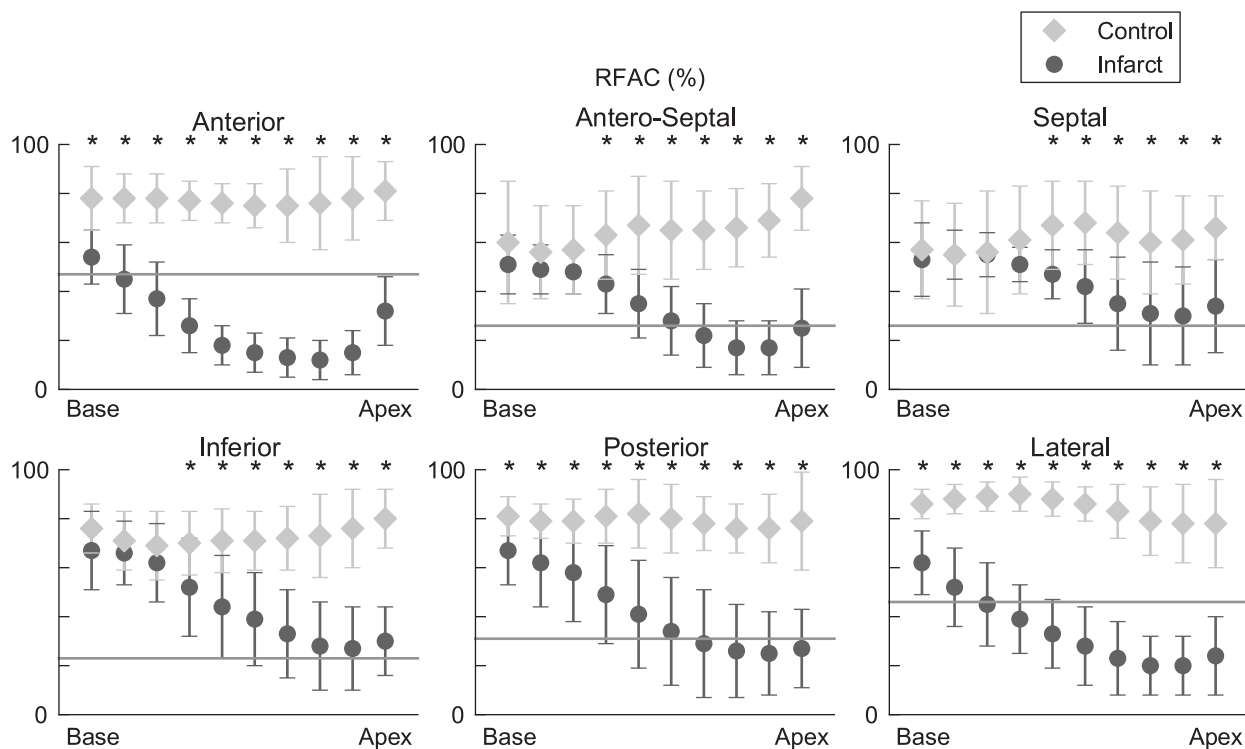


Fig. 4. Regional fractional area change (RFAC, mean values \pm SD) in control (gray squares) and infarcted (black dots) mice every 10% of LV length from base to apex ($*p < 0.05$, unpaired *t*-test). For each sector, the gray line shows the computed regional RFAC cut-off value for abnormality.

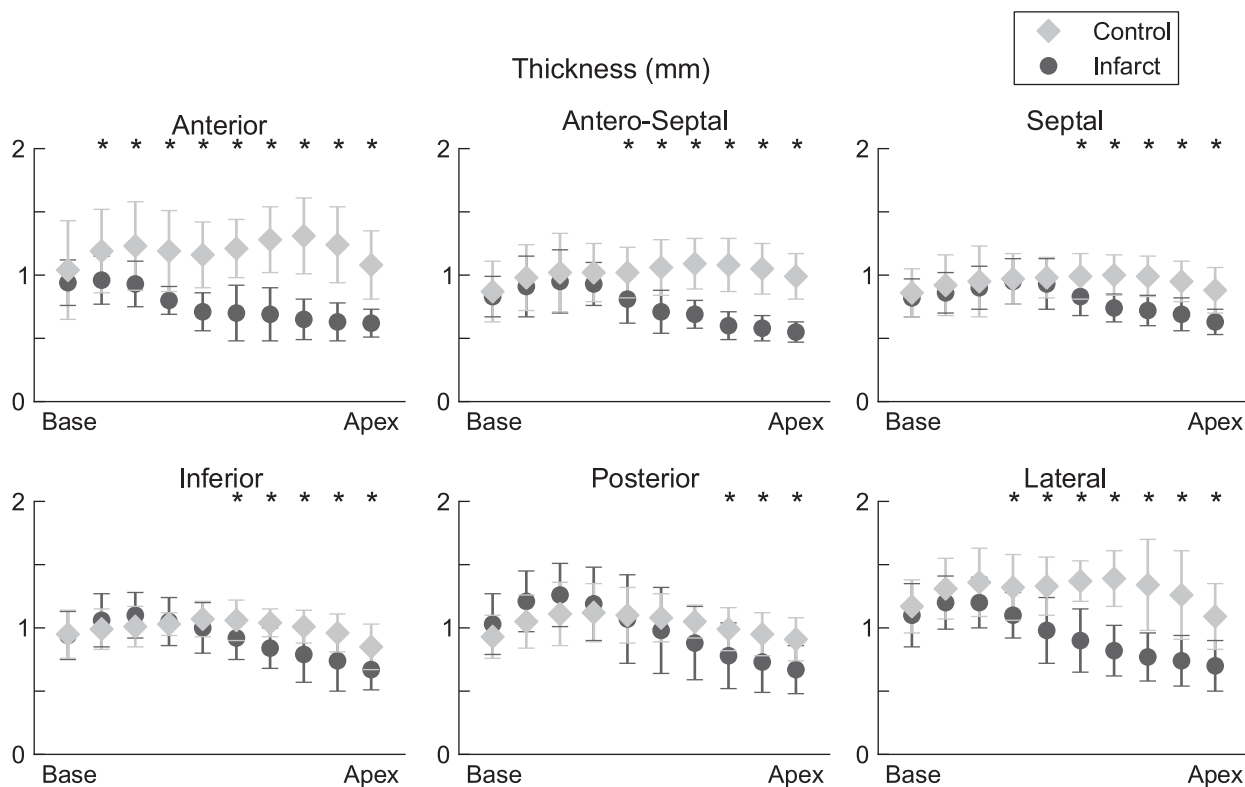


Fig. 5. LV wall thickness (mean values \pm SD) in control (gray squares) and infarcted (black dots) mice every 10% of LV length from base to apex ($*p < 0.05$, unpaired *t*-test).

To allow the easy visualization and comparison of the regional results obtained in all animals, the mean RFAC and LV thickness were displayed in bull's eye format, where values lower than the regional cut-off thresholds are represented with bold black contours (Fig. 6). In the C group, the RFAC values were

heterogeneous, with a maximum in the mid-lateral segment (90%) and a minimum in the basal septal segment (55%). The LV thickness also varied, with the maximum in the mid-lateral segment (1.39 mm) and the minimum in the apical inferior segment (0.85 mm). In the MMMI mice, RFAC and LV thickness

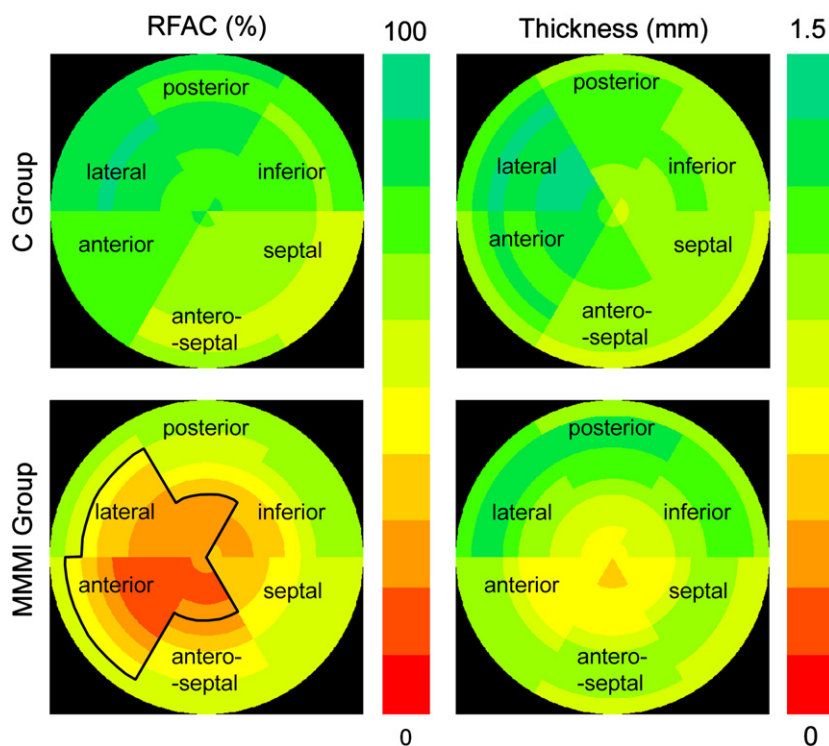


Fig. 6. Bull's eye representations of mean regional fractional area change (RFAC, left) and mean LV wall thickness (right) in the control (C, top) and infarcted (MMMI, bottom) mice. The slices from the LV apex to base are shown from the inner to the outer circle. The red and the green tones indicate lower and higher values, respectively: the corresponding scales are shown as color bars beside the panels. Bold black contour on the 'bull's eye' evidences those sectors in which the mean RFAC values were lower than the corresponding regional cut-off thresholds.

were lower in all of the mid- and apical-sectors, with the minimum RFAC (12%) in the anterior segment and minimum LV thickness in the apical antero-septal segment (0.55 mm). The anterior sector resulted to be the most extensively damaged, as indicated by the decrease in both RFAC and LV thickness from base to apex, due to the infarction induced by LAD ligation. In addition, sectors adjacent to the anterior one (i.e., lateral and antero-septal) showed a depressed RFAC, with mean values below the corresponding regional normality threshold, and reduced LV thickness at mid-apical level.

4. Discussion

Cine MR with retrospective gating has been shown to obtain high-quality heart images independently of ECG recording difficulties in high magnetic fields [19], also in mice with ECG-gating failure secondary to myocardial infarction [9]. This method makes ECG leads and respiratory sensors redundant, and has the distinct advantage that a steady-state longitudinal magnetization is maintained, resulting in almost constant LV wall signal intensity throughout the cardiac cycle. The main pitfall is that this is achieved at the expense of a decrease in the overall signal-to-noise ratio and contrast-to-noise ratio between blood and myocardial wall, as noted previously [8].

Images obtained by cine MR with retrospective gating can be used to extract global functional heart parameters, such as EDV, ESV, SV and EF. However, the applicability of this imaging technique for the automated evaluation of regional wall motion has not yet been tested [8].

In fact, current applications in murine evaluation of regional LV function are based on more complex MR sequences [12,13] that potentially allow the computation of 3D intra-myocardial strain, but on the other side require longer acquisition time, and

are limited by the maximal achievable tag spacing dimensions dependent of the technical capabilities of the scanner and the available radio-frequency coils. Moreover, in MMMI, because of the thinning of the infarcted wall, only a limited number of tags can be analyzed in the infarcted region, thus limiting the space resolution of the measurements.

We hypothesized that temporal and spatial resolution achieved with cine MR with retrospective gating could be sufficiently high to allow the quantification of not only global indices of LV function and mass, but also of frame-by-frame regional LV chamber areas, from which potentially detect wall motion abnormalities. The selected index on which the automated interpretation of wall motion was based, RFAC, was previously shown to be able to accurately reflect transitory worsening in regional endocardial LV wall motion in pigs, decreasing significantly in ischemic segments and being restored with reperfusion, in agreement with fluorescent microspheres validation [20]. Moreover, it was shown to allow accurate, fully automated, immediate, objective and experience-independent interpretation of regional LV function when compared to multiple-observer interpretation of cardiac MR images in humans [17].

Our choice to set threshold values of RFAC for normal and abnormal endocardial wall motion interpretation based on optimal values resulting from ROC analysis with the interpretation of the histological samples was based on the fact that in experiments involving an acute MI setting, measurement of the infarcted area in tissue sections of the LV is a standard approach to determine infarct size [21]. The application of these thresholds to C mice demonstrated their ability in correctly interpreting normal wall motion.

The regional analysis and bull's eyes representations of the MMMI mice made it possible to characterise the extent of myocardial damage in more detail. Compared to the C group, a reduction in RFAC extended to all of the LV sectors at mid- and

apical-levels, also in the basal anterior, posterior and lateral sectors, was noticed, despite the fact that only the LAD coronary artery was ligated (see Fig. 4). This finding is in agreement with that of Yang et al. [24], where LV contractile dysfunction was found early after large MI in mice, not only in the infarcted and adjacent segments, but also in the remote segments.

However, automated interpretation of RFAC showed abnormal segments localized from base to apex in the anterior and lateral segment, and apically in the surrounding sectors. In addition, a reduction in LV thickness at apical level and to different extents at different mid-level sectors (probably due to the replacement of necrotic by fibrous tissue) [22], was also found. The greatest reduction was observed in the anterior segment from base to apex, in correspondence with the greatest extent and magnitude of the reduction in RFAC found in the induced infarct model, in agreement with [23,24].

Using tagged MR in a rat model of myocardial infarction, Thomas et al. [15] found at one week after MI that: (1) the infarcted region was defined by a thinned, akinetic wall; (2) the adjacent zone was defined as an akinetic region with normal wall thickness, immediately adjacent to the infarcted region; (3) the remote zone was characterized by a reduction in myocardial motion. Also, Epstein et al. [12] showed in a MMMI by tagged MR a pattern of reduced cardiac shortening that evidenced a relative size of the dysfunctional area increasing toward the apex, with intermediate values consistently seen in the adjacent zone. These results appear very similar to the pattern of RFAC and myocardial thickness we reported in Fig. 6, thus supporting our hypothesis that also cine MR can provide reliable evidence of location and extension of the LV infarcted area.

The computations of RFAC in the C group revealed different mean values in the six sectors, with a 35% difference between the maximum and minimum values. While it is not possible to determine how much of this apparent variability is due to the challenge of applying an expeditious 2D analysis to the complexities of 3D cardiac wall motion, it nevertheless supports our approach of applying six different regional thresholds for RFAC instead of only one to take into account baseline regional differences in LV function when proceeding into the evaluation of the effects of induced myocardial infarction. In agreement with our findings, Thomas et al. [15] using tagged MR reported in normal rats values of regional myocardial displacement that differed up to 50% between septal and lateral segments.

As concerns global LV parameters, in the MMMI group the LV cavity resulted dilated, with a reduction in EF, PER and PFR, and an increased LV mass. These global changes are in line with the expected effects of post-infarction cardiac remodeling [25]. Conversely, SV was similar between MMMI and C groups, in agreement with the preservation of the same level of cardiac output.

The results in global LV parameters obtained in our study in the C group were comparable and within ranges described in multiple previous papers [26–30] using perspective cine MR imaging: EDV: 30–65 μ l, ESV: 9–27 μ l, SV 21–37 μ l, EF 58–69% and LV mass 57–95 mg. For the MMMI group, although our LV volumes seemed to be smaller compared to previously reported results, probably due to the earlier timing of MR acquisition and the younger age of our mice, EF and LV mass were comparable [26,28–30].

5. Limitations

The current study is focused on developing quick and expedient methods for estimating regional ventricular function from 2D short-axis images of the murine heart; it is acknowledged that the functional data obtained from 2D RFAC is inherently less

accurate and less sensitive to subtle changes in regional endocardial function than the more rigorous MRI methods of directly measuring 3D intra-myocardial strain by HARP or DENSE. Images spatial resolution was limited by technological restrictions.

6. Conclusions

In conclusion, cine MR imaging with retrospective gating potentially allows the regional quantification of LV function in mice. Regional LV wall motion interpretation and bull's eye display allowed the non-invasive localization of the extent of the induced infarction, and could be applied in studies assessing the effectiveness of pharmacological treatments or regenerative medicine in small animals.

7. Summary

7.1. Background

Magnetic resonance (MR) imaging is the method of choice for the left ventricular (LV) volumetric quantification of cardiac function in mice. Our purpose was to test the feasibility of using cine MR images acquired with retrospective gating to quantify not only global but also regional LV function in mice with myocardial infarction, using semi-automated quantification analysis tools, comparing the results with histological “gold standard”.

7.2. Methods

37 female C57BL6 mice with myocardial infarction (MMMI) induced by ligation of the left anterior descending (LAD) coronary were imaged (4.7 T scanner with retrospective gating) nine days after surgery. In 7 of them, histological analysis for hematoxylin and eosin staining was performed, and infarcted LV sectors identified, constituting the “gold standard” interpretation. Cine MR images were analyzed by custom software to compute regional fractional area change (RFAC). ROC analysis with histologic results was performed to determine the optimal RFAC cut-off values to detect infarcted segments, which were then applied to the remaining MMMI in order to describe the effects of ischemic injury on global and regional LV function and mass, and to a control group of 10 sham mice (C).

7.3. Results

Different RFAC cut-off values were found for each of the six LV sectors, with higher values associated to anterior (47%) and lower to inferior (23%) sectors. The application of these thresholds to C mice demonstrated their ability in correctly interpreting normal wall motion (98% accuracy). In MMMI, RFAC progressively decreased from base to apex, thus leading to significantly lower values in the anterior, posterior and lateral sectors throughout the LV compared to C. The anterior sector resulted to be the most extensively damaged (RFAC: 12%) by the infarction induced by LAD ligation. Also, adjacent sectors (lateral and antero-septal) showed a depressed RFAC, with mean values below the normality threshold.

7.4. Conclusions

Cine MR imaging with retrospective gating potentially allows the regional quantification of LV function in mice. Automated regional LV wall motion interpretation and bull's eye display allow the non-invasive localization of the extent of the induced

infarction, and could be applied in future studies assessing the effectiveness of pharmacological treatments or regenerative medicine in small animals.

Conflict of interest statement

None declared.

Acknowledgments

This study was supported in part by a Grant from Italian Ministry of Health and Monzino Cardiologic Center (Ricerca Finalizzata CCM-2007–669127).

References

- [1] R.I. Levy, J. Moskowitz, Cardiovascular research: decades of progress, a decade of promise, *Science* 217 (1982) 121–129.
- [2] L. Monassier, A. Constantinesco, Cardiovascular disorders: insights into in-vivo cardiovascular phenotyping, in: M.H. De Agelis, P. Chambon, S. Brown (Eds.), *Standards of Mouse Model Phenotyping*, Wiley VCH, Weinheim, 2006, pp. 177–199.
- [3] H.A. Brage, M. Ericsson, J.G. Seland, T. Pavlin, Ø. Ellingsen, C. Brekken, A comparison of retrospectively self-gated magnetic resonance imaging and high-frequency echocardiography for characterization of left ventricular function in mice, *Lab. Anim.* 45 (2011) 31–37.
- [4] J. Ruff, F. Wiesmann, K.H. Hiller, S. Voll, M. von Kienlin, W.R. Bauer, E. Rommel, S. Neubauer, A. Haase, Magnetic resonance microimaging for noninvasive quantification of myocardial function and mass in the mouse, *Magn. Reson. Med.* 40 (1998) 43–48.
- [5] R.G. Weiss, S.M. Chacko, F. Aresta, V.P. Chacko, Dynamic magnetic resonance images of murine cardiac function at physiological heart rates, *Circulation* 101 (2000) e92.
- [6] F. Wiesmann, J. Ruff, K.H. Hiller, E. Rommel, A. Haase, S. Neubauer, Developmental changes of cardiac function and mass assessed with MRI in neonatal, juvenile, and adult mice, *Am. J. Physiol. Heart Circ. Physiol.* 278 (2000) H652–H657.
- [7] J. Bishop, A. Feintuch, N.A. Bock, B. Nieman, J. Dazai, L. Davidson, R.M. Henkelman, Retrospective gating for mouse cardiac MRI, *Magn. Reson. Med.* 55 (2006) 472–477.
- [8] E. Heijman, W. de Graff, P. Niessen, A. Nauwerth, G. van Eys, L. de Graff, K. Nicolay, G.J. Strijkers, Comparison between prospective and retrospective triggering for mouse cardiac MRI, *NMR Biomed.* 20 (2007) 439–447.
- [9] B. Hiba, N. Richard, H. Thibault, M. Janier, Cardiac and respiratory self-gated cine MRI in the mouse: comparison between radial and rectilinear techniques at 7 T, *Magn. Reson. Med.* 58 (2007) 745–753.
- [10] R.C. Semelka, E. Tomei, S. Wagner, J. Mayo, G. Caputo, M. O'Sullivan, W.W. Parmley, K. Chatterjee, C. Wolfe, C.B. Higgins, Interstudy reproducibility of dimensional and functional measurements between cine magnetic resonance studies in the morphologically abnormal left ventricle, *Am. Heart J.* 119 (1990) 1367–1373.
- [11] M.S. Florentine, C.L. Grosskreutz, W. Chang, J.A. Hartnett, V.D. Dunn, J.C. Ehrhardt, S.R. Fleagle, S.M. Collins, M.L. Marcus, D.J. Skorton, Measurement of left ventricular mass in vivo using gated nuclear magnetic resonance imaging, *J. Am. Coll. Cardiol.* 8 (1986) 107–112.
- [12] F.H. Epstein, Z. Yang, W.D. Gilson, S.S. Berr, C.M. Kramer, B.A. French, MR tagging early after myocardial infarction in mice demonstrates contractile dysfunction in adjacent and remote regions, *Magn. Reson. Med.* 48 (2002) 399–403.
- [13] A.H. Aletras, S. Ding, R.S. Balaban, H. Wen, DENSE: displacement encoding with stimulated echoes in cardiac functional MRI, *J. Magn. Reson.* 137 (1999) 247–252.
- [14] W.D. Gilson, D.L. Kraitchman, Cardiac magnetic resonance imaging in small rodents using clinical 1.5 T and 3.0 T scanners, *Methods* 43 (2007) 35–45.
- [15] D. Thomas, V.A. Ferrari, M. Janik, D.H. Kim, S. Pickup, J.D. Glickson, R. Zhou, Quantitative assessment of regional myocardial function in a rat model of myocardial infarction using tagged MRI, *J. Magn. Magn. Mater.* 17 (2004) 179–187.
- [16] O. Tarnavski, J.R. McMullen, M. Schinke, Q. Nie, S. Kong, S. Izumo, Mouse cardiac surgery: comprehensive techniques for the generation of mouse models of human diseases and their application for genomic studies, *Physiol. Genomics* 16 (2004) 349–360.
- [17] E.G. Caiani, E. Toledo, P. MacEneaney, D. Bardo, S. Cerutti, R.M. Lang, V. Mor-Avi, Automated interpretation of regional left ventricular wall motion from cardiac magnetic resonance images, *J. Cardiovasc. Magn. Res.* 8 (2006) 427–433.
- [18] W.J. Manning, J.Y. Wei, S.E. Katz, S.E. Litwin, P.S. Douglas, In vivo assessment of LV mass in mice using high frequency cardiac ultrasound: necropsy validation, *Am. J. Physiol. Heart Circ. Physiol.* 266 (1994) 1672–1675.
- [19] B. Hiba, N. Richard, M. Janier, P. Croisille, Cardiac and respiratory self-gating cine MRI in the mouse at 7 T, *Magn. Reson. Med.* 55 (2006) 506–513.
- [20] V. Mor-Avi, E.G. Caiani, K.A. Collins, C.E. Korcarz, J.E. Bednarz, R.M. Lang, Combined assessment of myocardial perfusion and regional left ventricular function by analysis of contrast-enhanced power modulation images, *Circulation* 104 (2001) 352–357.
- [21] N. Ojha, S. Roy, J. Radtke, O. Simonetti, S. Gnyawali, J.L. Zweier, P. Kuppusamy, C.K. Sen, Characterization of the structural and functional changes in the myocardium following focal ischemia-reperfusion injury, *Am. J. Physiol. Heart Circ. Physiol.* 294 (2008) 2435–2443.
- [22] F. Yang, Y.-H. Liu, X.-P. Yang, J. Xu, A. Kapke, O.A. Carretero, Myocardial infarction and cardiac remodeling in mice, *Exp. Physiol.* 87 (2002) 547–555.
- [23] D. Kumar, T. Hacker, J. Buck, L.F. Whittessell, E.H. Keji, P.S. Douglas, T.J. Kamp, Distinct mouse coronary and myocardial infarction consequence to ligation, *Coron. Artery Dis.* 16 (2005) 41–44.
- [24] Z. Yang, S.S. Berr, W.D. Gilson, M.C. Toufektsian, B.A. French, Simultaneous evaluation of infarct size and cardiac function in intact mice by contrast-enhanced cardiac magnetic resonance imaging, reveals contractile dysfunction in noninfarcted regions early after myocardial infarction, *Circulation* 109 (2004) 1161–1167.
- [25] M. Nahrendorf, K.H. Hiller, K. Hu, G. Ertl, A. Haase, W.R. Bauer, Cardiac magnetic resonance imaging in small animal models of human heart failure, *Med. Image Anal.* 7 (2003) 369–375.
- [26] D. Dawson, C.A. Lygate, J. Saunders, J.E. Schneider, X. Ye, K. Hulbert, J.A. Noble, S. Neubauer, Quantitative 3-dimensional echocardiography for accurate and rapid cardiac phenotype characterization in mice, *Circulation* 110 (2004) 1632–1637.
- [27] P. Croisille, C. Rotaru, M. Janier, B. Hiba, Gender and strain variations in left ventricular cardiac function and mass determined with magnetic resonance imaging at 7 T in adult mice, *Invest. Radiol.* 42 (2007) 1–7.
- [28] L. Stegger, E. Heijman, K.P. Schäfers, K. Nicolay, M.A. Schäfers, G. Strijkers, Quantification of left ventricular volumes and ejection fraction in mice using PET, compared with MRI, *J. Nucl. Med.* 50 (2009) 132–138.
- [29] J.E. Schneider, P.J. Cassidy, C. Lygate, D.J. Tyler, F. Wiesmann, S.M. Grieve, K. Hulbert, K. Clarke, S. Neubauer, Fast, high-resolution in vivo cine magnetic resonance imaging in normal and failing mouse hearts on a vertical 11.7 T system, *J. Magn. Res. Imaging* 18 (2003) 691–701.
- [30] F. Wiesmann, J. Ruff, S. Engelhardt, L. Hein, C. Dienesch, A. Leupold, L. Illinger, A. Frydrychowicz, K.H. Hiller, E. Rommel, A. Haase, M.J. Lohse, S. Neubauer, Dobutamine-stress magnetic resonance microimaging in mice: acute changes of cardiac geometry and function in normal and failing murine hearts, *Circulation Res.* 88 (2001) 563–569.